DOI: 10.61782/fa.2023.0609

forum acusticum 2023

A CELLO BOWING PLAYBACK DEVICE? MOTION CAPTURE MEETS ROBOTIC ARM

Montserrat Pàmies-Vilà[1*] **Ewa Matusiak**[1] **Vasileios Chatziioannou**[1] **Alexander Mayer**[1]

[1] Department of Music Acoustics – Wiener Klangstil (IWK),
mdw – University of Music and Performing Arts Vienna, Vienna, Austria

ABSTRACT

The interaction between the bow and the bowed string has been analysed through numerous experimental and theoretical approaches, including the use of artificial bowing setups. In this study, with the objective of providing an experimental setup in which the string is bowed under realistic conditions, a robotic arm is used to reproduce the bow motion during cello playing. The first step of the methodology is to record the motion of the bow using optical motion capture. To that aim, an experienced cellist performs using a bow equipped with reflective markers while the cello is fixed on a platform. The recorded 3D motion of the bow, i.e., its position and inclination during playing, is then transformed into the coordinate system of the robotic arm. Hence, the robot can be instructed to reproduce the trajectories of the bow. Several bowing patterns, including various articulation techniques, have been reproduced using this approach. The current paper analyses the adequacy of this methodology for the study of cello bowing techniques.

Keywords: *bowed strings, bowing setup, music acoustics, artificial excitation*

1. INTRODUCTION

Motivated by the complex non-linear excitation at the contact point between the bow and the string, bowed-string instruments have been extensively studied in the field of music acoustics [1]. To that aim, many bowing devices have existed (or exist) that seek to evaluate the acoustics of bowed strings under laboratory conditions [2–7]. Since the first bowing devices —like the one by Raman in 1918 [2] and later by Schelleng [3]—, such setups have aimed at understanding sound production, initially at steady state and later during the production of transients [6, 7]. Using those devices, the goal was to achieve controlled playing conditions, which often required reducing the nuances of the player's action to a constant value in the playing parameters. Schoonderwaldt [5] experimented with articulation styles using a computer-controlled bowing machine with a monochord to explore the effect of bowing manipulations on the timbre of the violin. Other humanoid-like playing machines have been used for artistic or research purposes, demonstrating again the possibility of reproducing bowed sounds using a mechanical device [8, 9]. Nevertheless, these machines were not designed to produce realistically bowed sounds under controlled conditions.

After contributions by Schelleng [3], which showed that there is a narrow set of playing parameters that create a stable Helmholtz motion (given in the so-called *Schelleng diagrams* [1]), several studies have focused on the control parameters, i.e., the physical parameters that players change to control the produced sound [10–14]. Since the velocity of the bow is a key control parameter (together with the bow-string contact position and the bow force [14, 15]), such studies used motion capture to follow the trajectory of the bow, the instrument and the player's arms during performance. Motion capture systems are widely used to study the gestures of musicians when playing an instrument [16]. As such, motion capture has been used to track player and instrument movements during vi-

*__Corresponding author__: pamies-vila@mdw.ac.at.

olin performance [14, 17] and cello performance [18, 19].

In a previous study, we used a robotic arm to compare linear bowing trajectories to human slow-varying bowing motion [20]. The findings indicated a significant difference between the player's action and the robotic straight-line motion. In this study, we present an approach that aims to reproduce the motion of the bow as it was previously recorded with a real cello player. The goal of such a setup is to be able to analyse the playing nuances (such as articulation, bowing direction changes, and bowing adaptation to certain musical situations) in controlled laboratory conditions. To obtain the player's bowing action, motion capture technology is used to track the 3D movement of the bow, and a robotic arm is instructed with the recorded data in order to reproduce the bow motion.

2. MATERIALS AND METHODS

The present study compares human vs. robotic bowing on a cello that is mounted on a playing table. A beginner-level 4/4 cello with a cello bow, both by instrument retailer Thomann, are used. A robotic arm and a motion capture system are set as follows.

2.1 Robotic arm

A robotic arm by Universal Robots (model UR5e) is used in this study. It weighs 20.6 kg and has a reach of 850 mm, with a maximum holding capacity of 5 kg. The robot consists of six joints, providing six degrees of freedom and, thus, all possible positions and angles within its reach. A custom-made 3D-printed clamp is used to fix the frog of the bow to the holding joint of the robot, the centre of which is usually referred to as Tool-Center-Point TCP, as seen in Figure 1.

The tool holds the bow and moves it according to the TCP coordinates, which are given by its 3D spatial location relative to the base of the robot $\{\boldsymbol{R}\}$, as indicated in Figure 2. This spatial location is given as 3 positions and 3 angles. The positions are given in the metric system, and the angles are given in axis-angle representation. Alternatively, the six joint angles can be individually modified. For the purpose of this research, the robot is externally driven through a real-time data-transfer (RTDE) protocol [21]. This approach allows sending robot coordinates with a frame rate of up to 500 Hz.

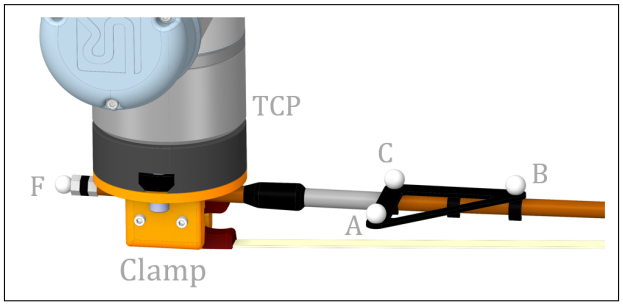

Figure 1: Custom-made clamp that attaches the bow to the robot holding joint. Indication of the position of the reflective markers on the frog (F) and on the wood of the bow (A, B, C).

2.2 Motion capture

The motion capture setup consists of 12 infrared cameras (Optitrack Prime 13) operating at a frame rate of 240 fps. These cameras are set to send and receive infrared light that is reflected from the reflective markers located at selected places (i.e. affixed to an instrument or to the bodies of the performers). Five reflective markers are placed on the bow, while some reference markers are placed on the corpus of the cello, on the playing platform and, if necessary, on selected players' body parts. On the bow, one marker is placed on the tip, one on the frog and three markers are placed in between them. As seen in Figure 1, a triangular 3D-printed mount is used to clamp three markers on the wood of the bow. This triangular arrangement might be used to calculate the rotations (in axis-angle representation) of the bow.

2.3 Conversion and communication between systems

From the motion capture recording, data coordinates in 3D are obtained that represent the X, Y, and Z positions of all markers in the recording space. The camera coordinate frame $\{\boldsymbol{C}\}$ indicates the origin of the motion-capture space, which is placed on the surface of the platform, in front of the instrument and next to the robot (marked with $\{\boldsymbol{C}\}$ in Figures 2 and 3). All motion-capture data are originally given in relation to this coordinate frame $\{\boldsymbol{C}\}$. The first processing step happens in the motion-capture software (Motive by Optitrack), in which every marker is assigned a label and, if necessary, possible occlusions are interpolated. After exporting the motion-capture data of the bow-markers (markers F, A, B, C, T), all 3D data are

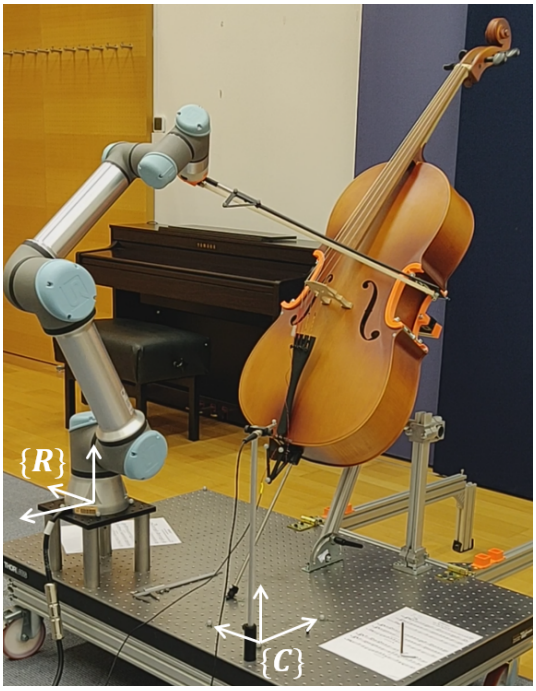

Figure 2: Image of the robot on the playing platform and the cello mounted on the holding structure. Indication of the motion-capture coordinate frame $\{\boldsymbol{C}\}$ (defining the ground plane) and the robot coordinate frame $\{\boldsymbol{R}\}$ (defining the robot world frame).

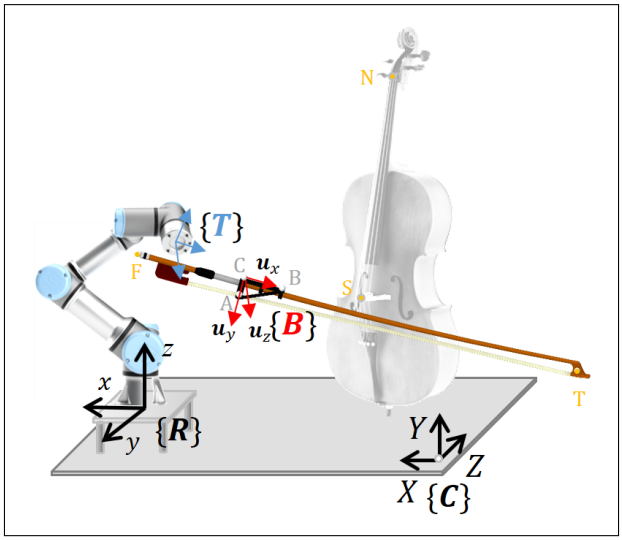

Figure 3: Indication of the motion-capture coordinate frame $\{\boldsymbol{C}\}$, the robot coordinate frame $\{\boldsymbol{R}\}$, the location of the bow frame $\{\boldsymbol{B}\}$ and the tool frame $\{\boldsymbol{T}\}$, as well as the location of the bow-markers F, A, B, C, T and cello-markers S, N. Exaggerated proportions for better visualisation.

then converted to the robot coordinate frame $\{\boldsymbol{R}\}$ via a change of basis. The robot coordinate frame $\{\boldsymbol{R}\}$ is the so-called world frame of the robot, defining the origin of all data that interact with the robot. We also use the robot world frame $\{\boldsymbol{R}\}$ as the origin of the data for the rest of the paper. At this point, the unit vectors $\mathbf{u}_x$, $\mathbf{u}_y$ and $\mathbf{u}_z$ are calculated using the bow markers. These unit vectors define the bow coordinate frame $\{\boldsymbol{B}\}$. The next step is the alignment of the bow frame $\{\boldsymbol{B}\}$ and the TCP frame $\{\boldsymbol{T}\}$ (the centre point of the holding joint), again with a change of basis. This implies a translation and a rotation of $\{\boldsymbol{B}\}$ to get $\{\boldsymbol{T}\}$. From the TCP frame $\{\boldsymbol{T}\}$, we obtain the rotation matrix, i.e. the orientation of the object at all times with respect to the world frame $\{\boldsymbol{R}\}$. This rotation matrix is used to calculate the axis-angle representation, as required by the robot software. The axis-angle representation is expressed as $[r_x, r_y, r_z] = \theta\mathbf{a}$, where θ and $\mathbf{a}$ are the angle and the vector, respectively, that give the orientation of the bow. Finally, the six robot coordinates are obtained at each time instance: three positions and three angles $[x_\mathrm{r}, y_\mathrm{r}, z_\mathrm{r}, r_x, r_y, r_z]$. With fast changes in the given position and orientation, the robot recreates the recorded motion of the bow.

The original motion-capture data is exported in a CSV file containing the X, Y, Z positions of the required markers in the $\{\boldsymbol{C}\}$ frame. These data were used without any filtering for the purpose of data transfer to the robot. After the aforementioned geometrical conversion (implemented in Matlab), the frame rate is interpolated from 240 Hz (motion-capture rate) to 250 Hz (giving a time interval of 0.004 s for the robot instructions). A series of robot coordinates is exported to a txt file as $[x_\mathrm{r}^n, y_\mathrm{r}^n, z_\mathrm{r}^n, r_x^n, r_y^n, r_z^n]$, at every time-step n. This file is used for data transfer to the robot.

The communication with the robot happens via the Universal Robots Real-Time Data Exchange (RTDE) protocol [21], using the software LabVIEW by National Instruments. A graphical user interface (GUI) is used to visualise and control the data transfer and the recordings. The current version of this software ensures the correct transfer of the coordinates at 250 Hz, updating the robot coordinates every 0.004 s. The receiving robot program

performs the inverse kinematics conversion in real time on the internal computer of the robotic arm. This executes the conversion from the positions and angles of the TCP to the angles of the robot joints. Simultaneously, the robot TCP coordinates and joint angles are received and displayed in the GUI. The user has the option to adjust the offset settings for the three TCP position values (x, y, z), as well as to select different sending modes, including playing through in real time, step-through with a slider, and autoplay loop mode. The GUI may also display the current position of the robot's TCP and its joint angles. Although at this step the position offsets can be adapted, for the purpose of the present research, no extra modifications have been applied, and the used data are given only considering the motion-capture recording and the conversion algorithm.

2.4 Experimental procedure

The recordings consisted of synchronised measurements of motion capture and sound using a microphone RG50 by ROGA Instruments with a sampling rate of 44100 Hz, as well as a piezoelectric sensor attached to the side of the cello bridge. Additional video images were recorded to facilitate the data analysis.

One advanced cello player was invited to play several open-string exercises (i.e. without fingering any notes with the left hand) using the prepared instrument and bow. The cello was mounted on a steady holding structure on top of a playing platform and could not be moved (Figure 2). The position of the cello was determined after a study with six cellists, which considered their height and body proportions and evaluated their comfort during playing [22]. In the present study, the cellist could not adapt the position of the cello (nor its inclination or the length of the spike), but they could adapt the height and position of the seat, as well as their sitting position on the setup, to achieve better comfort or reach.

After data conversion (Sec. 2.3), the robot was instructed to reproduce the bow motion. Using the same recording setup as for the musician, the 3D trajectories of the robot-driven bow were recorded again (motion capture, audio and video data). The data shown in this paper were recorded with an interval of two weeks between the sessions.

In this paper, two repetitions at different dynamics are shown. All strings were played 8 times using half-notes at 100 bpm; once at piano dynamics and once at mezzo-forte dynamics. The player followed a metronome click and could decide the loudness of the dynamic indications. The study protocol was approved by the Ethics Committee of the University of Music and Performing Arts Vienna.

2.5 Data conditioning

The data that are shown in this paper regard the motion of the frog marker F and compare the human-playing (red) with the robot-playing conditions (blue). This marker has been chosen for its proximity to the player's hand. All other markers showed similar results, with a slightly higher error in the tip marker because of the flexibility of the bow and possible oscillation of the bow tip. For the purpose of these plots, the data were filtered using a Butterworth 3$^{\text{rd}}$ order filter at 12 Hz to reduce measurement noise. In this study, the marker positions x, y, z are given with respect to the robot coordinate frame $\{\boldsymbol{R}\}$. This implies that when the player bows 'to their right' (down bow), x increases, and when the player bows 'to their left' (up bow), x decreases. The z coordinate is vertical (positive upwards), and the y coordinate grows to the front and diminishes to the back.

3. RESULTS

To compare the performances of the human player and the robotic arm, the marker at the frog F is used to compute several parameters. The x, y, z positions of this marker, together with its velocity on each axis (with respect to the robot world frame $\{\boldsymbol{R}\}$) are shown in Figure 4. This figure shows a segment of an exercise where 8 bow strokes were played on each string, at piano dynamics, from high to low pitch. The figure shows five bow strokes on the D_3 string and five bow strokes on the G_2 string. The bow motion achieved by the robotic arm (blue) is very similar to the human motion (red), overlapping on these plots most of the time. The mean error between the two signals is close to zero for all three coordinates, showing no significant offset in any direction. However, some discrepancies are observed at the bow change, i.e., when the bow quickly reverses direction, changing from up-bow to down-bow. At these instants, the maximum error between the signals is 4 mm, with the robot always achieving a slightly shorter range of motion than the human. This shows that the robot action acts like a low-pass filter, since the most brusque bow changes or fast changes of velocity are performed slower by the robot than by the human performer. This can also be observed in the velocity plots (right of Figure 4), where the fastest changes (from $+200$ mm/s to

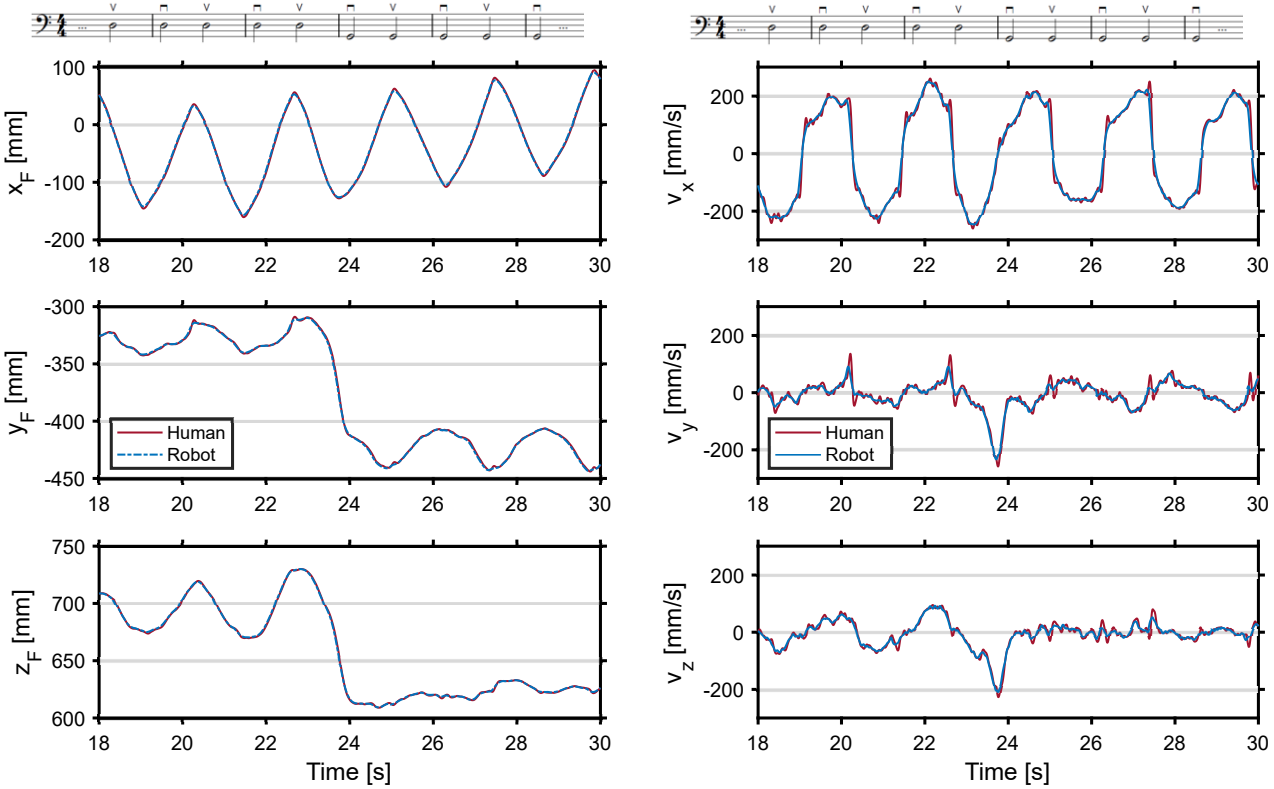

Figure 4: Three positions (x_F,y_F,z_F) and their first derivative (v_x,v_y,v_z), comparing the player's bow movement (red) and the robot's bow movement (blue) as displayed by the marker placed on the frog of the bow (F in Figure 1). At $t \approx 24$ s there is a change from the D_3 string to the G_2 string. Down-bow ($\sqcap$) and up-bow ($\vee$) are indicated at the top. Note that the left-plots are not in the same scale (x_F shows a 300 mm span, while y_F and z_F show a 150 span).

-150 mm/s in v_x) are performed at a slightly lower velocity by the robot. Nevertheless, the comparison shows that the robot achieves the same level of bow velocity in all three axes, as well as most of the characteristics of the velocity profile that are observed in the player signals.

At the bottom of Figure 5, the recorded sound pressure of the played open-string exercise is shown, comparing the human and the robotic players. Every bow stroke is repeated eight times on every string (four times down-bow and four times up-bow). It is shown that both human (red) and robot (blue) play at the given dynamics: first softer (*p*) and later louder (*mf*). This is due to the wider range of the bow motion at the given tempo, as seen in the x_F plot (x-coordinate of the frog marker F, top of Figure 5). A wider range of motion of the bow results in a faster velocity at the bow-string contact point and, thus, a louder sound. These sound signals show that the best match between human and robot performance is achieved at the third played string (G_2), and the worst is given at the first string (A_3). To evaluate this issue, the middle plot shows the calculated minimum distance between the frog-tip line of the bow markers (F, T in Figure 3) and the bridge-nut line of the cello (S and N in Figure 3), hereafter σ_contact. This is calculated as the minimum geometrical distance between two lines in the 3D space. The parameter σ_contact gives an indication of the inaccuracies that might show up at the bow-string contact, and it is used to assess the performance of the robot focusing at the contact point of the bow on the string. Since there are only two markers on the cello (at the middle of the bridge and at the middle of the nut), the parameter σ_contact is expected to change slightly at each string. A higher σ_contact in the robot per-

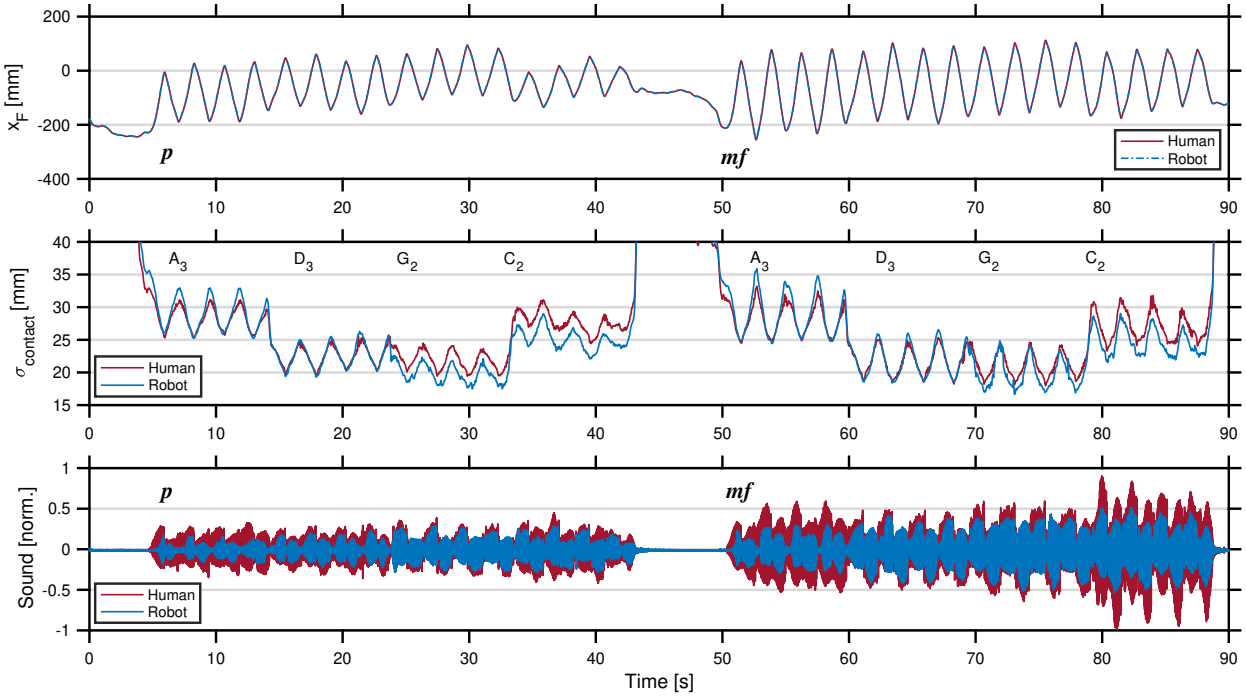

Figure 5: Two repetitions of the open-string exercise at piano dynamics (*p*, softer) and at mezzo-forte dynamics (*mf*, louder). The x-coordinate of the frog marker x_{F} shows the main direction of bowing. $\sigma_{\mathrm{contact}}$ shows the minimum distance from the Frog-Tip line to the Bridge-Nut line. At the bottom, a comparison of the recorded sound pressure achieved by the human player (red) and by the robotic arm (blue).

formance compared to the human performance indicates that the bow is not being pressed enough on the string, or is too far away from the string. This is the case of the first string (A_3), where the robot-bow-position is slightly further away from the string than the human-bow-position, at both dynamics (*p* and *mf*). This might result in a light bow-string contact or even in a bow position that does not touch the string (e.g. at the beginning of the first note of the recording). The second string D_3 shows the best match in $\sigma_{\mathrm{contact}}$, as well as a good match in sound in mezzo-forte dynamics, but not in piano dynamics. For the third string (G_2) the best match in sound is observed, yet the robot-signal appears at a lower $\sigma_{\mathrm{contact}}$ (around 2 mm). This indicates that the robotic setup might require an adjustment at a shorter $\sigma_{\mathrm{contact}}$ than the human to compensate for the differences in the playing situation (absence of a human behind the instrument, absence of damping at the right hand, or possible accumulated errors during the conversion process). A similar situation happens on the lowest string (C_2). The fact that the match in $\sigma_{\mathrm{contact}}$ depends on the played string might indicate an error in the measurement of the angles between the bow-frame $\{\boldsymbol{B}\}$ and the tool-frame $\{\boldsymbol{T}\}$.

4. DISCUSSION

The results of this study indicate that the proposed method to convert 3D motion-capture data of the bow motion to 3D robotic instructions achieves accurate reproduction of the velocities of the bow, but its position is highly dependent on many geometrical parameters in the conversion process. As such, small errors in the calculation of the parameters of the change of basis between the camera base and the robot base might at last result in a noticeable error in the position of the bow. Similarly, inaccuracies in

the measurement of the dimensions of the bow and its distance to the robot tool might also result in an offset of the data in some axis or an inaccurate angle of inclination of the bow. For instance, it is not straightforward to measure the angles of rotation that might be needed between the camera and world frames, as well as the angle of rotation between the bow frame and the tool frame. These issues add to the accuracy of the motion-capture system, which showed mean errors of 0.51 mm and 0.42 mm during the human-player and robot-player recordings, respectively. Although the cello was kept on the same table and position, changes in the position of the nut-marker N of up to 3 mm in the x axis have been observed. Changes on the cello markers might indicate that the presence of the person behind the cello does slightly modify its position (the chest presses against it), or that the position of the cello was slightly modified between recordings due to unknown reasons.

This paper shows that there is a limitation in the performance of very fast direction changes, like the ones present at the bow change (from up-bow to down-bow and vice versa), resulting in a position error of up to +/- 4 mm, and a smaller velocity peak (Figure 4) at these instances. These errors depend on the speed of the bow, showing higher errors for fast bow changes, and lower errors for slower changes in the bow motion. The robot was used with the standard 'restricted' safety configuration, which limits the speed of the robot tool to 1500 mm/s. The velocities in the tested motions did not reach this limit. A change to the least restricted safety configuration (tool speed limit of 5000 mm/s) did not show an improvement in the bow-change limitations described here.

It has been observed that, despite the above-mentioned error accumulation, the robot motion as quantified by the frog marker resembles very much the motion of the human player. Nevertheless, proper sound generation might not always be achieved. As seen in the bottom of Figure 5, the difference in the recorded sound between human and robot is still string dependent, with better results for the G and D strings (the middle strings), than for the C (lowest) and the A (highest) strings, particularly at mezzo-forte dynamics. Future research should consider the bowing pressure to adapt to the small errors present in the proposed method, which are mainly due to geometrical inaccuracies. An extended setup that reacts to the forces that take place at the bow-string contact would also allow adapting to a different cello position or eventually to a different bow or cello.

5. CONCLUSION

A cello bowing playback device based on a robotic arm can substantially benefit from the recordings of a motion capture system. The 3D recording of the human performance, particularly the motion of the bow, is a necessary step to instruct the robot to follow these human-like trajectories while playing. The current research uses optical motion capture to achieve this task. The study has shown that the robotic arm can achieve similar bow motions as the original recording with a human-player. Possible sources of error have been explored, and it has been attempted to minimise them. The current state of this methodology still shows errors up to 4 mm in the 3D position, which are particularly high at the bow-change. If these errors are found on an axis that moves the bow further away from the cello, they might result in the absence of adequate bow-string contact. Nonetheless, the presented methodology achieves a bow-string contact or a position very close to a bow-string contact in all four strings, with successful reproduction of the played sounds in the central strings of the cello.

6. ACKNOWLEDGEMENTS

The authors would like to acknowledge Anna Scheiblauer for her support during the recordings. This research was funded in whole, or in part, by the Austrian Science Fund (FWF) [T1259-G, P34852-N].

7. REFERENCES

[1] T. Rossing, *The Science of String Instruments*. New York: Springer, 2010.

[2] C. V. Raman, "On the mechanical theory of the vibrations of bowed strings and of musical instruments of the violin family, with experimental verification of the results, part i.," *Indian Association for the Cultivation of Science*, vol. 15, pp. 243–276, 1918.

[3] J. C. Schelleng, "The bowed string and the player," *The Journal of the Acoustical Society of America*, vol. 53, no. 1, pp. 26–41, 1973.

[4] A. Cronhjort, "A computer-controlled bowing machine (mums)," *Speech, Music and Hearing Quarterly Progress and Status Report*, vol. 33, no. 2-3, pp. 61–66, 1992.

[5] E. Schoonderwaldt, "The violinist's sound palette: spectral centroid, pitch flattening and anomalous low

frequencies," *Acta Acustica united with Acustica*, vol. 95, no. 5, pp. 901–914, 2009.

[6] P. Galluzzo and J. Woodhouse, "High-performance bowing machine tests of bowed-string transients," *Acta Acustica united with Acustica*, vol. 100, no. 1, pp. 139–153, 2014.

[7] R. Mores, "Precise cello bowing pendulum," *Proc. 3rd Vienna Talk on Music Acoustics*, vol. 106, 2015.

[8] S. Jordà, "Afasia: the ultimate homeric one-man-multimedia-band," in *Proc. NIME*, (Dublin), 2002.

[9] K. Shibuya, S. Matsuda, and A. Takahara, "Toward developing a violin playing robot-bowing by anthropomorphic robot arm and sound analysis," in *Proc. 16th IEEE Int. Symposium on Robot and Human Interactive Communication*, pp. 763–768, 2007.

[10] A. Askenfelt, "Measurement of bow motion and bow force in violin playing," *The Journal of the Acoustical Society of America*, vol. 80, no. 4, pp. 1007–1015, 1986.

[11] A. Askenfelt, "Measurement of the bowing parameters in violin playing. ii: Bow–bridge distance, dynamic range, and limits of bow force," *The Journal of the Acoustical Society of America*, vol. 86, no. 2, pp. 503–516, 1989.

[12] M. Demoucron, *On the control of virtual violins-Physical modelling and control of bowed string instruments*. PhD thesis, Université Pierre et Marie Curie - Paris VI; Royal Institute of Technology, Stockholm, 2008.

[13] E. Maestre, *Modeling instrumental gestures: an analysis/synthesis framework for violin bowing*. PhD thesis, Department of Information and Communication Technologies, Universitat Pompeu Fabra, Barcelona, 2009.

[14] E. Schoonderwaldt and M. Demoucron, "Extraction of bowing parameters from violin performance combining motion capture and sensors," *The Journal of the Acoustical Society of America*, vol. 126, no. 5, pp. 2695–2708, 2009.

[15] A. Lampis, A. Mayer, M. Pàmies-Vilà, and V. Chatziioannou, "Examination of the static and dynamic bridge force components of a bowed string," in *Proc. of Meetings on Acoustics*, 2023.

[16] M. M. Wanderley, "Motion capture of music performances," in *The Oxford Handbook of Music Performance* (G. E. McPherson, ed.), pp. 465–494, Oxford University Press, 2022.

[17] J. Van Der Linden, E. Schoonderwaldt, J. Bird, and R. Johnson, "Musicjacket—combining motion capture and vibrotactile feedback to teach violin bowing," *IEEE Transactions on Instrumentation and Measurement*, vol. 60, no. 1, pp. 104–113, 2010.

[18] J. Rozé, M. Aramaki, R. Kronland-Martinet, and S. Ystad, "Exploring the perceived harshness of cello sounds by morphing and synthesis techniques," *The Journal of the Acoustical Society of America*, vol. 141, no. 3, pp. 2121–2136, 2017.

[19] T. Wofford, *Study of the interaction between the musician and the instrument. Application to the playability of the cello*. PhD thesis, Sorbonne Université, Paris, 2018.

[20] M. Pàmies-Vilà, A. Scheiblauer, A. Mayer, and V. Chatziioannou, "A framework for the analysis of bowing actions with increased realisticness," in *Proc. of the 24th International Congress on Acoustics*, vol. 437.

[21] A. Mayer, M. Pàmies-Vilà, and V. Chatziioannou, "The Universal Robots Real-Time Data Exchange (RTDE) and LabVIEW," tech. rep., Department of Music Acoustics - Wiener Klangstil (IWK), 2022.

[22] A. Scheiblauer, A. Mayer, and M. Pàmies-Vilà, "Investigating the cello position, bow motion and cellist posture using motion capture," in *Proceedings of Meetings on Acoustics, Fourth Vienna Talk on Music Acoustics*, vol. 49, p. 035013, Acoustical Society of America, 2022.